Journal of Analytical and Applied Pyrolysis 151 (2020) 104919

Contents lists available at ScienceDirect

Journal of Analytical and Applied Pyrolysis

journal homepage: www.elsevier.com/locate/jaap

Quantitative NMR analysis of the aqueous phase from hydrothermal liquefaction of lignin

Hilde V. Halleraker *, Tanja Barth

Department of Chemistry, University of Bergen, Allégaten 41, 5007 Bergen, Norway

ARTICLE INFO

Keywords:
Hydrothermal liquefaction
Lignin to liquid
Lignin
Quantitative NMR

ABSTRACT

Hydrothermal liquefaction (HTL) of biomass such as lignin could contribute to finding replacements for petroleum, both as a fuel and production of chemicals. The organic phase produced in formic acid assisted HTL of lignin has been extensively analyzed previously. The solid phase is routinely analyzed by elemental analysis, and the gas phase has also been studied. The aqueous phase, on the other hand, has received little attention so far and this paper aims to identify and quantify the organic compounds that remain in the aqueous phase after the workup of the organic phase. Using NMR with water suppression, this is achieved with simple sample preparation. The major components are identified using 2D NMR (HSQC spectra) together with proton spectra and ^{13}C spectra as well as verification with standard samples. Their concentrations are determined based on ^{1}H spectra with an added internal standard. An initial evaluation of the effect of temperature and catalyst in the formic acid assisted HTL is given to demonstrate the relevance of the approach. Methanol, formic acid, acetic acid, acetone, phenol, catechol, and dimethyl ether have been identified and quantified in aqueous samples from six different HTL-experiments. 76 %–86 % of the peak area of the proton spectra have been accounted for.

1. Introduction

Finding replacements for petroleum products is important both because of the depletion of petroleum resources and the increased focus on the reduction of greenhouse gas emissions. Lignin is the most abundant renewable source of aromatics, with its intricate polymer structure derived from phenolic monomers, and could therefore be a valuable raw material for making chemicals that are currently being produced from petroleum. A promising process in this respect is the lignin to liquid solvolysis (LtL), which, in essence, is a formic acid assisted hydrothermal liquefaction (HTL) [1]. In this process, lignin, solvent, and formic acid are placed in a reactor to be heated at temperatures in the range of 280 °C – 380 °C. The formic acid will mainly function as a hydrogen donor in the process, though some of the carbon from formic acid also reacts in the process and becomes part of the oil [2]. Formic acid assisted HTL produces an organic phase, often referred to as bio-oil, together with a gas phase, an aqueous phase, and char. The organic phase has been extensively studied [3–5], and the char is routinely analyzed by elemental analysis. The gas phase has also been analyzed in some studies [4,6]. The aqueous phase from formic acid assisted HTL, on the other hand, has previously only been qualitatively analyzed in one case [7]. It is therefore of interest to investigate the compounds that remain in the aqueous phase after liquid-liquid extraction, both qualitatively and quantitatively. These compounds can play a role in the depolymerization reactions of the lignin and conversion of carbohydrate residues in partially purified lignin feedstocks, as well as possibly providing an additional product if extracted and purified. Finally, they will be a factor in terms of waste management at large scale. One possibility for waste management is to use the aqueous phase for biogas production. There are studies that investigate the recycling of the aqueous phase for use as solvent in the continuous HTL reaction, which report an increase in bio-oil yield in experiments with various whole biomasses [8–10]. However, in one case where lignin was used as feedstock, the bio-oil yield decreased when the aqueous phase was recycled [8]. Thus, knowledge of the precise composition of the organic compounds in the water phase are important for understanding the thermochemical reaction pathways and optimizing the process conditions to give a maximum value product slate.

Aqueous phases can be difficult to analyze for their content of highly water-soluble molecules. GC—MS (gas chromatography-mass spectrometry) is most often used. However, sample preparation, such as derivatization or extraction, can be quite extensive in order to optimize

* Corresponding author.
E-mail address: hilde.v.halleraker@uib.no (H.V. Halleraker).

https://doi.org/10.1016/j.jaap.2020.104919
Received 6 May 2020; Received in revised form 3 August 2020; Accepted 1 September 2020
Available online 6 September 2020

Table 1
Experimental conditions.

Experiment	Lignin g	Water g	Formic acid g	Temperature °C	Time h	Type of catalyst	Reactor size
350 °C-NoCatalyst	200	400	244	350	2	No catalyst	5 L
350 °C-Goethite	200	400	244	350	2	Goethite	5 L
350 °C-Ru/Al	200	400	244	350	2	Ruthenium/ Alumina	5 L
305 °C-NoCatalyst	200	400	244	305	2	No catalyst	5 L
305 °C-Goethite	200	400	244	305	2	Goethite	5 L
305 °C-Ru/Al	200	400	244	305	2	Ruthenium/ Alumina	5 L
Blank	0	7.4	3.66	360	2	No catalyst	75 mL

the properties of the samples for GC- analysis [11–13], which can result in lower accuracy. Aqueous samples can also be analyzed by GC—MS using the purge-and-trap technique as well as by the much simpler headspace analysis, but only the volatile components of the sample will be extracted by these methods [11]. Some studies have nonetheless used GC—MS to analyze aqueous phases [8,12,14]. They report phenols as the compound group with the highest concentration in the aqueous phase from HTL of lignin both with and without recycling of the aqueous phase. Organic acids were also detected in the aqueous phase, and a higher concentration of organic acids was observed when the aqueous phase was recycled [8]. Liquid chromatographic analysis, including ion chromatography, has also been used for the analysis of water-soluble organic molecules [15–17], but the separation capacity and sensitivity are not satisfactory for all the relevant molecules. When using GC and HPLC (high-performance liquid chromatography) for quantification, calibration curves need to be prepared because equal concentration of different analytes usually results in different detector responses [18].

NMR spectroscopy has developed into an alternative approach for the analysis of complex mixtures and molecules with no physical separation of the components required. The use of NMR spectroscopy in the analysis of bio-oil has been established as a useful method to procure information on functional groups within the bio-oil [2,19–21]. Pure shift NMR has been developed as a method to simplify the elucidation of structures in complex mixtures such as bio-oils, using a data processing approach where the proton spectrum is simplified to eliminate the multiplicity of a peak leaving a single peak for each signal [22,23]. Using NMR spectroscopy to analyze aqueous samples eliminates issues with separation of the sample as well as complicated sample preparation. Additionally, the use of calibration curves is unnecessary when using NMR since proton NMR can be easily acquired with quantitative parameters where the peak area is directly proportional to the number of protons that creates a given peak in the spectrum [24–27]. Aqueous samples from the thermochemical conversion of biomass, as analyzed in this study, comprise a quite simple mixture of compounds, which makes their conclusive identification possible. Quantification of the compounds in the aqueous phase using NMR spectroscopy is simple and reliable when using an internal standard as a reference [27,28]. Quantitative NMR (qNMR) spectroscopy is a well-established technique in several research fields, for instance vaccines and drugs as well as food and beverages [25,29,30]. Process water from hydrothermal carbonization (HTC) of furfural residue, which is a solid residue mainly composed of cellulose and lignin, has been analyzed using NMR spectroscopy. 5-hydroxymethylfurfural, glycerol, formic acid, methanol, acetic acid, levulinic acid, hydroxyacetone, and acetaldehyde were identified and quantified from the process water from HTC [30]. NMR spectroscopy has, to our knowledge, not been utilized in quantitative analysis of the aqueous phase from HTL of lignin, making this a novel approach to resolve the issue of analyzing the aqueous phase from lignin solvolysis.

The aim of this paper is to identify and quantify the organic compounds in the aqueous phase of HTL of lignin using NMR with water suppression. The set of samples used in this investigation has been generated at different temperatures and with different catalysts, and the effect of these parameters on the amounts and composition of the aqueous compounds is also evaluated.

2. Experimental

2.1. Formic acid assisted hydrothermal liquefaction

The lignin conversion was done in a 5 L reactor (high-pressure autoclave reactor from ESTANIT GmbH) at the conditions listed in Table 1. All the experiments were performed with stirring. The results regarding oil yield from the HTL-experiments are reported elsewhere [31]. The aqueous phase from these experiments is the basis for the analysis in this work. The feedstock, termed lignin throughout this paper, is a lignin-rich residue from weak acid and enzymatic hydrolysis of Eucalyptus wood. It was produced in Örnsköldsvik in Sweden at the Biorefinery Demo Plant. Based on elemental analysis (C: 4.17 mol%, H: 5.87 mol%, N: 0.03 mol%, O: 2.45 mol%), the lignin content of the feedstock was estimated to be approximately 50 wt.%. According to protocol NREL/TP-510−42622, the ash content was determined to be approximately 4.4 wt.%. The catalysts, Ruthenium/Alumina (batch no. Lot #10714KYV, catalogue no. 381152, Ru mass fraction 5 %) and goethite (batch no. Lot #BCBQ8228 V, catalogue no. 71063, Fe mass fraction 30–63 %), were purchased from Sigma-Aldrich. Description of the workup of the conversion products can be found elsewhere [31]. The ratio between lignin, water, and formic acid is based on experiments performed at laboratory scale with reactor size of 25 mL to make the experiments at different scales comparable. A blank experiment was conducted in a 75 mL reactor from Parr instruments. The experimental conditions are listed in Table 1.

2.2. NMR spectroscopy of aqueous sample

2.2.1. Sample preparation

The samples were diluted by taking 4.000 mL of aqueous sample and adding 4.000 mL distilled water, using an Eppendorf pipette. 0.400 mL internal standard, 2.125 M of dimethyl sulfone, was added with an Eppendorf pipette to the diluted aqueous sample. pH was measured before 8.400 mL of a buffer solution with pH 7.4 was added using an Eppendorf pipette (0.010 M $Na_2HPO_4 \cdot 2\,H_2O$ with 20 % D_2O containing TSP salt), and the pH was adjusted to 7.4 using 1.0 M NaOH. The pH-adjustment was done to ensure reproducible chemical shifts and to prevent resonance influence by acidic protons [28]. The sample was filtered before 600 μL was transferred to an NMR-tube. The precipitate that formed during sample preparation was collected as the solution was filtered through a filter paper using a Büchner funnel. Dimethyl sulfone (standard for quantitative NMR), sodium phosphate dibasic dihydrate ($Na_2HPO_4 \cdot 2\,H_2O$), and deuterium oxide (containing 0.05 wt.% TSP salt) were all purchased from Sigma-Aldrich and used without further upgrading.

2.2.2. NMR parameters

Proton spectra for quantification, noesygppr1d, were performed on a 600 MHz Bruker AVANCE NEO NMR-spectrometer equipped with a QCI CryoProbe with four RF channels with a 30 ppm spectral width and 8 scans together with a relaxation time of 50 s. The probe temperature was 25 °C.

Carbon spectra, zgpg30, and deptqgpsp, as well as the 2D spectra, were performed on an 850 MHz Bruker Avance III HD NMR-

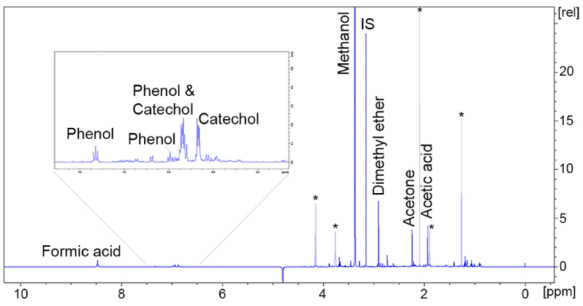

Fig. 1. Proton spectrum of the aqueous phase of experiment 350 °C-NoCatalyst. IS is internal standard dimethyl sulfone. The peaks marked with * are solvent peaks remaining from previous extraction of the aqueous phase with ethyl acetate and THF. Enlargement of the area between 0 ppm and 5 ppm can be found in Fig. S1 in supplementary material.

spectrometer equipped with a TCI CryoProbe. The zgpg30 and deptqgpsp were acquired with a spectral width of 239 ppm, 768 scans, and 262k points. The 2D hsqc spectra were acquired in non-uniform-sampling mode with a spectral width of 16 ppm and 165 ppm for proton and ^{13}C, respectively, 1024 points for proton and 256 points for carbon. Proton spectra used for elucidation of structures, noesygppr1d, were also performed on the 850 MHz Bruker Avance III HD NMR-spectrometer. The spectral with was 30 ppm with 32 number of scans and a relaxation time of 4 s.

TopSpin 4.0.7 (Bruker BioSpin) was used in the analysis of the obtained spectra.

2.3. Infra-Red spectroscopy of the precipitate

The samples were applied to an attenuated total reflectance crystal, and FT-IR spectra were recorded by a Nicolet iS50. The spectral range was 4000 cm^{-1} to 400 cm^{-1} with a resolution of 4 cm^{-1}, and the number of scans was 32. The software OMNIC 9.8.286 (Thermo Scientific inc.) was used to obtain and analyze the spectra.

2.4. Elemental analysis of the precipitate

Elemental analysis was performed on a Vario EL III instrument from Elementar, which is an elemental analyzer for simultaneous carbon, hydrogen, nitrogen, and sulfur analysis. In this case, the instrumentation is not calibrated for sulfur. Acetanilide was used to calibrate the instrument.

2.5. Principal component analysis

Principal component analysis (PCA) is a widely used statistical method that extracts the systematic information from a data set and expresses that information as a set of principal components, which is variables that are orthogonal to each other. The first principal component explains most of the variance in the dataset. The second component must be orthogonal to the first component and explain as much of the variance in the dataset as possible under that constraint. PCA simplifies the description of the dataset as well as compresses the size of the dataset by only retaining the important information [32]. This technique has been utilized in this study to explore the relationship between the compositional data of the dissolved organic compounds and the reaction conditions. Since this is a study of screening experiments, PCA can be used to evaluate the relative importance of the experimental factors and visualize correlations that will otherwise be overlooked even though this is a relatively small dataset [33]. Sirius 10.0 by Biomar AS was used for the statistical analysis.

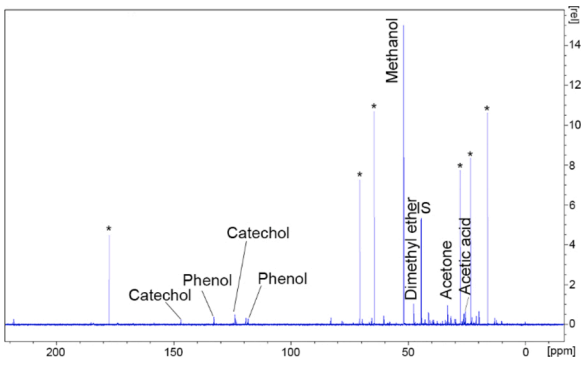

Fig. 2. ^{13}C spectrum of the aqueous phase of experiment 350 °C-NoCatalyst. IS is internal standard dimethyl sulfone. The peaks marked with * are solvent peaks from extraction with ethyl acetate and THF. Enlargement of the area between 0 ppm and 100 ppm can be found in Fig. S2 in supplementary material.

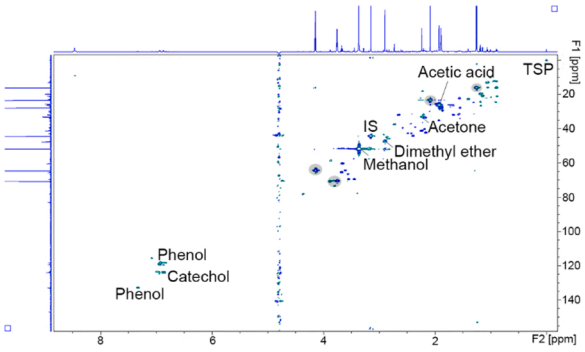

Fig. 3. HSQC spectrum of the aqueous phase of experiment 350 °C-NoCatalyst (the peaks marked in grey are THF and ethyl acetate from extraction). IS is internal standard dimethyl sulfone. A larger version of this spectrum can be found in supplementary material Fig. S3.

3. Results and discussion

3.1. NMR-analysis of the aqueous samples – identification of compounds

Figs. 1–3 shows a representative proton spectrum, a ^{13}C spectrum, and a 2D plot of a representative aqueous phase produced in HTL conversion of lignin to bio-oil. The most prominent peak in all the proton spectra occurs at δ 3.37 ppm and is assigned to methanol, based on the findings of Løhre et al. [28] and verified by analysis of the cross-peaks in the obtained 2D-spectra [34]. The other identified compounds are acetic acid (δ 1.93 ppm) [28], acetone (δ 2.24 ppm), dimethyl ether (δ 2.90 ppm), catechol (δ 6.87 ppm, δ 6.95 ppm), phenol (δ 6.93 ppm, δ 6.99 ppm, δ 7.33 ppm), and formic acid (δ 8.47 ppm) [28]. Neither acetic acid nor formic acid shows the typical peak from the acidic proton, which is as expected since acidic protons are prone to be exchanged for deuterium from the solvent. This is also the case for the hydroxy proton on methanol. All the unidentified peaks in the area between 0.88 ppm and 4.46 ppm are organic molecules connected to an electronegative element such as oxygen, thus providing sufficient polarity for them to remain in the aqueous phase during workup. The most upfield peaks (around 1 ppm) could be from an aliphatic chain on an alcohol or another functional group containing oxygen. There are few literature values for chemical shift of organic molecules in water as solvent, making it difficult to deduce the structures of the remaining peaks. There are also some unidentified peaks in the area of aromatic proton (7−8 ppm). The blank experiment produced small amounts of methanol, formic acid, acetone, and dimethyl ether. Proton NMR of the aqueous phase from the blank experiment can be found in the supplementary material.

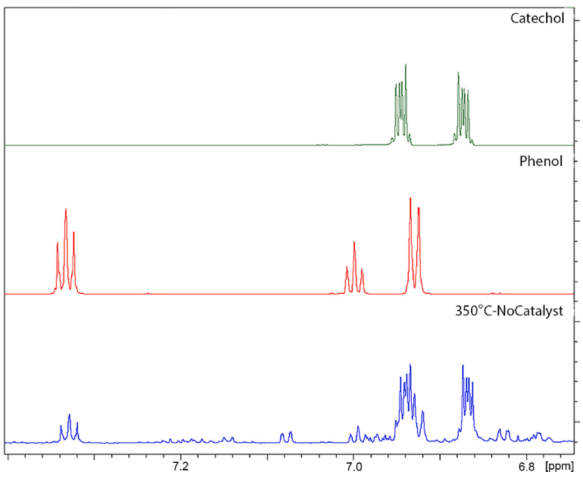

Fig. 4. Proton NMR-spectra of Catechol (top), Phenol (middle), and the aqueous phase from experiment 350 °C-NoCatalyst (bottom), confirming the presence of Catechol and Phenol in the aqueous phase.

Table 2
Peak assignment for major peaks in Figs. 1 and 2.

Compound		^{1}H Chemical shift ppm	Number of protons		^{13}C chemical shift ppm
$DMSO_2$ (IS)	CH_3	3.16	6	CH_3	44.4
Acetic acid	CH_3	1.93	3	CH_3	26.1
Acetone	CH_3	2.24	6	CH_3	33.1
Dimethyl ether	CH_3	2.90	6	CH_3	47.6
Methanol	CH_3	3.37	3	CH_3	51.8
Catechol	Ph-H (position 4 & 5)	6.87	2	Aromatic C (position 3 & 6)	123.9
Catechol	Ph-H (position 3 & 6)	6.95[a]	2	Aromatic C (position 4 & 5)	146.9
Phenol	Ph-H (position 2 & 6)	6.93[a]	2	Aromatic C (position 2 & 6)	118.3
Phenol	Ph-H (position 4)	6.99	1	Aromatic C (position 3 & 5)	132.8
Phenol	Ph-H (position 3 & 5))	7.33	2	Aromatic C (position 4)	123.5
Formic acid	HCOOH	8.47	1		

[a] Overlapping signal, not used for quantification.

Fig. 2 shows the assigned peaks in the carbon spectrum of the same sample. Similar to what is seen in the proton spectrum, methanol provides the strongest signal in the carbon spectrum. The quaternary carbons in phenol and catechol were difficult to find amongst the noise in the spectrum, but the other signals in the aromatic section of the spectrum are assigned to phenol and catechol. Additionally, there are several small peaks in the range of 12 ppm–85 ppm in the carbon spectrum, which corresponds to carbon in alkanes and carbon connected by a single bond to oxygen, or other electronegative elements [35]. Since water is the solvent, the exact chemical shifts differ from spectra with DMSO or chloroform as solvents, making it challenging to utilize literature values obtained with those solvents to identify the peaks in the spectra presented here.

The HSQC spectrum in Fig. 3 is useful in verifying the identification of the structures. Methanol presents itself as the most prominent peak based on the methyl part of the molecule in both the proton spectra and the carbon spectra (3.37 ppm and 51.83 ppm, respectively), and the connection between those peaks is found in Fig. 3 verifying that the peaks are in fact from methanol.

There are some aromatic compounds present as well, with signals at 6.95 ppm and 6.87 ppm in the proton spectrum and 123.9 ppm and 118.3 ppm in the carbon spectrum. The largest peaks in the aromatic section of the proton spectra have been confirmed to be catechol and phenol by acquiring NMR-spectra of standard samples, as seen in Fig. 4. The peak at 2.90 ppm in the proton spectrum is identified as dimethyl ether based on the HSQC and HMBC spectra in combination with the proton and carbon spectra. The peaks in the 2D-spectra reveal a symmetric molecule where the proton at 2.90 ppm presents with a cross peak with carbon at 47.6 ppm in the HSQC (Fig. 3) proving a direct connection between the two atoms. The HMBC spectrum, which shows connections between atoms that are two or three bonds away from each other, also show a cross peak between the carbon at 47.6 ppm and the proton at 2.90 ppm. There are no other cross-peaks in the 2D-spectra associated with either the 2.90 ppm proton or the 47.6 ppm carbon. This information combined with the fact that the proton peak is a singlet, which means that there are no protons connected to an adjacent carbon, and that the chemical shifts are in the area of carbon that is connected to an electronegative atom such as oxygen, leads to the conclusion of this molecule being dimethyl ether. Dimethyl ether is a gas at room temperature but is fairly soluble in water [36]. A list of all the identified compounds and their observed proton shift values are given in Table 2.

3.2. *Quantification of the identified species*

Quantification of the identified compounds is based on the proton spectra and the number of protons in each peak. All the concentrations have been calculated using the internal standard, dimethyl sulfone, as reference. Fig. 4 shows the concentration of the identified compounds in the aqueous sample before dilution, and it is clear that methanol is the compound with the highest concentration in all the samples, which can also be seen in Table 3. Løhre et al. reported excellent reproducibility for this method with a relative standard deviation of less than 1 % (mM) [28]. The blank experiment, which was performed by only adding formic acid and water to the reactor, produced small amounts of acetone,

Table 3
Concentration of the identified compounds, given as milli Molar concentrations.

Experiment	Acetic acid mM	Acetone mM	Methanol mM	Formic acid mM	Phenol mM	Catechol mM	Dimethyl ether mM	Percentage of total peak area quantified
350 °C-NoCatalyst	52.54	5.131	578.1	75.49	0.9986	3.516	12.87	83 %
350 °C-Goethite	47.04	11.25	724.8	52.67	3.410	4.526	13.00	85 %
350 °C-Ru/Al	62.73	13.63	742.3	6.119	0.5312	1.264	9.558	84 %
305 °C-NoCatalyst	36.00	7.040	828.0	94.47	0.9455	15.57	18.75	86 %
305 °C-Goethite	13.97	6.895	782.1	87.01	1.200	5.843	17.92	86 %
305 °C-Ru/Al	72.23	8.616	626.4	11.83	0.2550	13.45	12.81	76 %
Blank	0	1.000	49.4	4.11	0	0	0.29	100 %

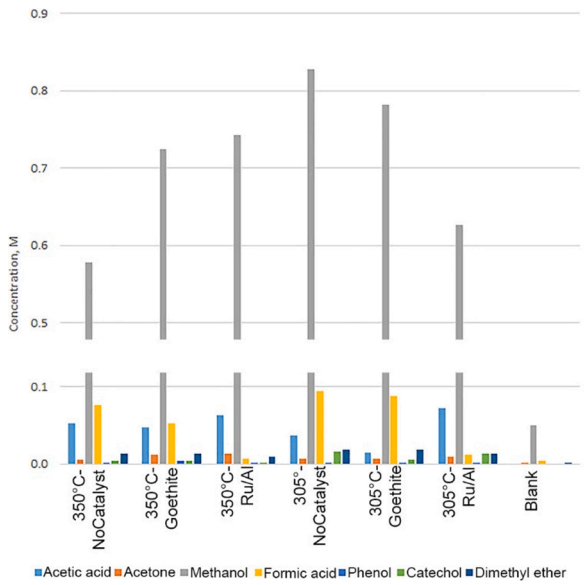

Fig. 5. Concentration of acetic acid, acetone, methanol, formic acid, phenol, catechol, and dimethyl ether in the aqueous samples before dilution, all values are given in Molar concentrations.

formic acid, methanol, and dimethyl ether, as seen in Table 3 and Fig. 5. The large amounts of those compounds produced in the other experiments can therefore not only be a result of decomposition of formic acid under the HLT conditions but is rather a result of the reaction between lignin and formic acid.

In addition to acetic acid, acetone, methanol, formic acid, dimethyl ether, phenol, and catechol, which have been identified and quantified, there are also organic solvents, tetrahydrofuran, and ethyl acetate, present in the aqueous phase, which have been introduced during liquid-liquid extraction in the workup of the conversion products. Additionally, small amounts of unidentified small organic compounds are dissolved in the aqueous phases. The production of −OH containing compounds in the HTL reaction performed here arises mostly from cleavage of ether bonds in lignin, possibly through a formylation reaction with subsequent elimination and hydrogenolysis with hydrogen from formic acid as described by Oregui-Bengoechea et al. [37]. There is a potential for the production of value-added chemicals from the organic acids found in the aqueous phases [14], although the concentrations in these samples are quite low. However, it is valuable information in a waste management perspective to know what the aqueous phase consists of and the concentration of the compounds. When we look at the total concentration of the quantified compounds, the experiment that has the lowest concentration of organic compounds is 350 °C-NoCatalyst, which means that this experiment is the most favorable in a waste management perspective. However, in order to tell which experiment is the most favorable overall, this must be seen in connection with which parameters result in the highest oil yield. As a general trend, Ghoreishi et al. found that increasing temperature leads to decreasing oil yield, meaning that 350° is not the most favorable temperature in terms of bulk oil yields. The Ruthenium/ Alumina experiments were the most efficient experiments with regards to high oil yields and low char yields [31]. The 305°-Ru/Al experiment is the second-best experiment in a waste management perspective, and one of the best experiments when it comes to oil yield and char yield.

To explore the relationship between the compositional data of the dissolved organic compounds and the reaction conditions, a principal component analysis (PCA) of the data has been performed. The results are shown in the biplot in Fig. 5.

Considering the biplot shown in Fig. 5, we can see which variables are correlated to each other either positively, negatively, or not at all. The PCA model that forms the basis for this biplot explains about 70 % of the variance in the dataset, which means that we can extract general trends from this analysis. Acetic acid is closely correlated to the Ruthenium/Alumina catalyst. Catechol is correlated to no catalyst and negatively correlated to temperature. Phenol is correlated to the goethite catalyst. Acetone is correlated to higher temperatures. The production of methanol is negatively correlated to the Ruthenium/Alumina catalyst and slightly positively correlated to the goethite catalyst. Formic acid is negatively correlated to the Ruthenium/Alumina catalyst, which is also clear from examining Fig. 4, where we see that the concentration of formic acid is greater in the experiments performed without catalyst and with the goethite catalyst compared with the experiments performed with the Ruthenium/Alumina catalyst.

The trends can be interpreted as a consequence of changes in the reaction pathways caused by the presence of the catalysts. Since the purpose of the catalysts is to enhance hydrodeoxygenation [38], the no catalyst experiment correlates with higher yields of more oxygenated species, and especially catechol. The thermal decomposition of formic acid to water and CO_2 is shown to be catalyzed by the Ruthenium/alumina catalyst, explaining the negative correlation. The other catalysts clearly also influence the reaction pathways for the lignin depolymerization, but a more detailed investigation is needed to elucidate the details of these processes.

In this work, the spectral resolution has been considered sufficient when using an 850 MHz magnet for the structural elucidation, deeming the pure shift approach described in the introduction not relevant. The multiplicity gives valuable information in structure elucidation and together with 2D spectra, we have accounted for 76 % - 86 % of the protons in the samples (see Table 3) based on the quantitative proton NMR. This gives us a good understanding of which organic compounds remain in the aqueous phase after the normal workup procedure following the hydrothermal liquefaction. Considerable work and skill will be required to identify and quantify the remaining minor peaks in the proton spectra.

Chen et al. report that there are large amounts of phenolic compounds in the aqueous phase from the HTL of lignin (at 350 °C for 60 min). They found phenol, guaiacol, and syringol using GC–MS and estimated those to be the most abundant species based on peak area [8]. This is not quite in agreement with our findings seeing as there are such low concentrations of the aromatic compounds in our samples. However, the workup procedure they used did not include liquid-liquid extraction of the aqueous phase which leaves more of the organic compounds in the aqueous phase. It is also worth keeping in mind that using the peak area of a gas chromatogram to estimate concentrations has its weaknesses since the response factor of different compounds can vary considerably, meaning that two compounds with the same concentration can result in considerably different peak areas. Chen et al. did not report finding any of the other compounds we found in our study. According to Madsen et al., the aqueous phase from HTL of whole biomass samples contained organic acids with acetic acid being the most abundant with concentrations of up to 0.087 M [14], which is comparable to the results from this study where we found concentrations between 0.014 M and 0.078 M of acetic acid. The analytical methods used by both Chen et al. and Madsen et al. will not be able to detect small organic molecules such as methanol and dimethyl ether since compounds with low boiling points are not detectable using standard GC–MS procedures. Yue et al. have analyzed aqueous phases from hydrothermal carbonization of biomass that are comparable to the samples presented here using NMR and found 5-HMF, formic acid, methanol, acetic acid, levulinic acid, glycerol, hydroxy acetone, and acetaldehyde at various concentration depending on reaction time and temperature. They concluded that most of the lignin in the reaction remained in the biochar, with only partial lignin decomposition into aliphatic and aromatic compounds [30]. Compared to the results presented here, it is reasonable to assume that some of the detected methanol, formic acid and acetic acid originates from the lignin fraction of the starting material.

Table 4
Color description of the samples and pH of the samples before sample preparation.

Experiment	pH before sample preparation	Color after sample preparation	Amount of precipitate after sample preparation (mg/mL)
350 °C-NoCatalyst	5.42	Brown/orange	2.03
350 °C-Goethite	5.50	Brown	2.08
350 °C-Ru/Al	6.55	Yellow	2.08
305 °C-NoCatalyst	4.43	Black	2.04
305 °C-Goethite	4.86	Black	3.28
305 °C-Ru/Al	5.05	Red	3.96

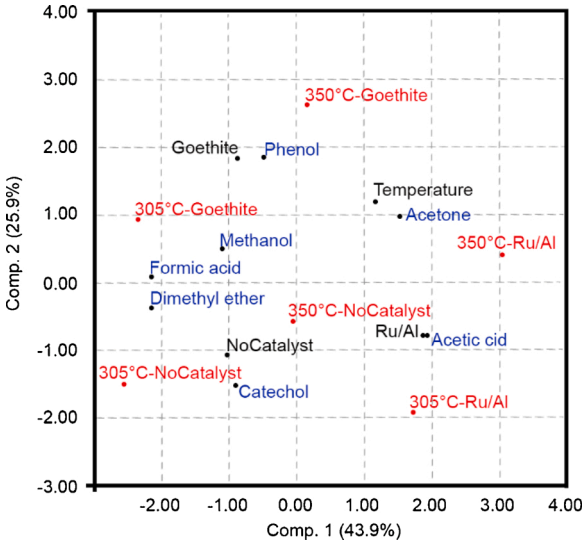

Fig. 6. Biplot containing all the experiments, all variables, and all the identified and quantified compounds from this work.

3.3. Description of the aqueous phases

The pH in the samples ranges from 4.43 to 6.55, as shown in Table 4, showing the presence of acids in the aqueous phases. After sample preparation with the addition of buffer solution and pH adjustment, the aqueous samples had different colors, as shown in Fig. 7 and described in Table 4. All the samples gave a precipitate as the pH was adjusted. Particles are observed in the samples before sample preparation, showing that storage affects the samples to some degree since the aqueous phase is filtered in the workup procedure of HTL from lignin

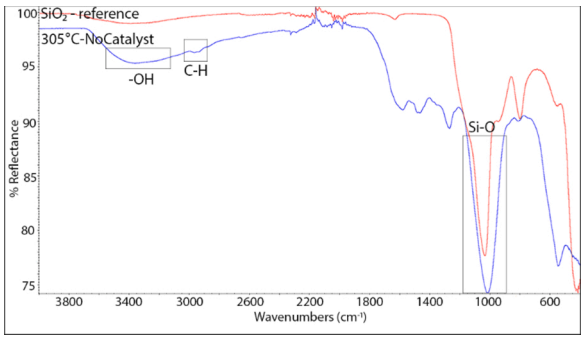

Fig. 8. IR-spectrum of experiment 305 °C-NoCatalyst (blue) compared to SiO_2 (red) as reference.

and thus does not contain any particles when the samples are placed in the refrigerator for storage. However, it was clear during the preparation of the aqueous samples for NMR-analysis that new precipitates were formed as well.

Table 4 includes information on how much precipitate is formed during sample preparation, which is in the range of 2.03 mg/mL to 3.96 mg/mL and seems to be somewhat dependent on temperature in the HTL reaction, meaning that lower temperatures favor more precipitate.

3.4. Characterization of the precipitate

The infra-red spectra (Fig. 8) revealed a substantial inorganic component in the precipitate, proven to be SiO_2 by the collection of a reference spectrum, with the peak at about 1000 cm^{-1}. The SiO_2 originates from the biomass ash, which has been determined to be about 4.4 % of the biomass. Kraft lignin from eucalyptus, which is comparable to the lignin used in this work, has been measured to contain 1100 mg silicon per kg dry lignin [39]. Additionally, there are some trace of organic components shown by the peaks at about 2900 cm^{-1}. The broad peak at about 3370 cm^{-1} is typical of −OH, which could either be from −OH connected to silicon or carbon or from residual water in the sample. However, the −OH peak is still present, but slightly less prominent after the sample had been dried at 70 °C for 24 h. The IR spectrum of experiment 305 °C-NoCatalyst is shown in Fig. 6. A spectrum comparing the eucalyptus lignin to the precipitate can be found in supplementary material, Fig. S4.

The elemental analysis measures hydrogen, carbon, and nitrogen, and although the instrument can measure sulfur, it has not been calibrated for sulfur. For organic samples, oxygen is normally calculated by difference, assuming that the rest of the sample is oxygen, however in this case, that would be incorrect since there are some inorganics in the sample as well. The elemental analysis revealed that the precipitate includes some hydrogen (up to 4.3 mol %) and carbon (up to 3.5 mol %) in addition to minute amounts of nitrogen (0.07 mol %). Up to 72 wt. %

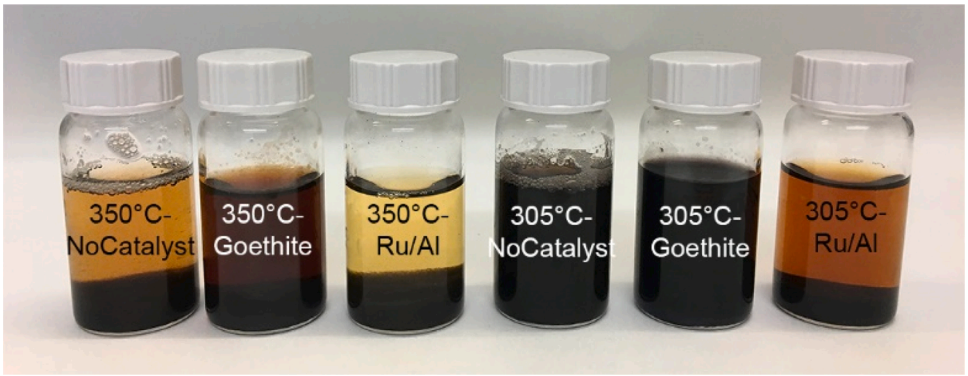

Fig. 7. Aqueous phases after sample preparation for NMR analysis. Solid precipitate can be observed in the vials.

of the samples are not measured in the analysis, meaning that there are substantial amounts of inorganics in the samples.

4. Conclusion

NMR analysis has proven to be a good method for quantitative analysis of aqueous samples from hydrothermal conversion of lignin, and we have successfully quantified 76 % – 86 % of the total peak area of the proton spectra. Acetic acid, acetone, methanol, formic acid, dimethyl ether, phenol, and catechol have been identified and quantified, and methanol is the compound with the highest concentration in the range of 0.58 M to 0.83 M. The low concentrations do not support recovery of the organic chemicals. In a waste management perspective, the most favorable conditions are 350 °C with no catalyst. Experiment 350 °C-NoCatalyst produces, in total, the lowest concentration of organic compounds that are retained in the aqueous phase after workup of solvolysis products. A precipitate formed during sample workup of the aqueous samples for NMR, which IR-analysis has proven to be mainly silicon oxide together with small amounts of organic compounds.

Funding

This work was partly supported by the Research Council of Norway through the Norwegian NMR Platform, NNP (226244/F50). The authors gratefully acknowledge the University of Bergen for funding Hilde V. Halleraker.

CRediT authorship contribution statement

Hilde V. Halleraker: Conceptualization, Methodology, Validation, Formal analysis, Investigation, Data curation, Writing - original draft, Writing - review & editing, Visualization. **Tanja Barth:** Conceptualization, Methodology, Validation, Resources, Writing - review & editing, Supervision, Project administration, Funding acquisition.

Declaration of Competing Interest

The authors report no declarations of interest.

Acknowledgment

The authors would like to thank I. J. Fjellanger for assisting with elemental analysis and J. Underhaug for assisting with the acquisition of NMR data. The authors would also like to thank S. Ghoreishi for providing the samples and the information on the experimental conditions.

Appendix A. Supplementary data

Supplementary material related to this article can be found, in the online version, at doi:https://doi.org/10.1016/j.jaap.2020.104919.

References

[1] L. Cao, C. Zhang, H. Chen, D.C.W. Tsang, G. Luo, S. Zhang, J. Chen, Hydrothermal liquefaction of agricultural and forestry wastes: state-of-the-art review and future prospects, Bioresour. Technol. 245 (2017) 1184–1193, https://doi.org/10.1016/j.biortech.2017.08.196.
[2] H.V. Halleraker, S. Ghoreishi, T. Barth, Investigating reaction pathways for formic acid and lignin at HTL conditions using 13C-labeled formic acid and 13C NMR, Results Chem. 2 (2020), 100019, https://doi.org/10.1016/j.rechem.2019.100019.
[3] G. Gellerstedt, J.B. Li, I. Eide, M. Kleinert, T. Barth, Chemical structures present in biofuel obtained from Lignin, Energy Fuels 22 (2008) 4240–4244, https://doi.org/10.1021/ef800402f.
[4] M. Oregui Bengoechea, A. Hertzberg, N. Miletić, P.L. Arias, T. Barth, Simultaneous catalytic de-polymerization and hydrodeoxygenation of lignin in water/formic acid media with Rh/Al2O3, Ru/Al2O3 and Pd/Al2O3 as bifunctional catalysts, J. Anal. Appl. Pyrolysis 113 (2015) 713–722, https://doi.org/10.1016/j.jaap.2015.04.020.
[5] C. Løhre, G.-A.A. Laugerud, W.J.J. Huijgen, T. Barth, Lignin-to-Liquid-Solvolysis (LtL) of organosolv extracted lignin, ACS Sustain. Chem. Eng. 6 (2018) 3102–3112, https://doi.org/10.1021/acssuschemeng.7b03057.
[6] B. Holmelid, M. Kleinert, T. Barth, Reactivity and reaction pathways in thermochemical treatment of selected lignin-like model compounds under hydrogen rich conditions, J. Anal. Appl. Pyrolysis 98 (2012) 37–44, https://doi.org/10.1016/j.jaap.2012.03.007.
[7] C. Løhre, H.V. Halleraker, T. Barth, Composition of lignin-to-Liquid solvolysis oils from lignin extracted in a semi-continuous organosolv process, Int. J. Mol. Sci. 18 (2017) 225, https://doi.org/10.3390/ijms18010225.
[8] H. Chen, Z. He, B. Zhang, H. Feng, S. Kandasamy, B. Wang, Effects of the aqueous phase recycling on bio-oil yield in hydrothermal liquefaction of Spirulina platensis, α-cellulose, and lignin, Energy 179 (2019) 1103–1113, https://doi.org/10.1016/j.energy.2019.04.184.
[9] C. Li, X. Yang, Z. Zhang, D. Zhou, L. Zhang, S. Zhang, J. Chen, Hydrothermal liquefaction of desert shrub Salix psammophila to high value-added chemicals and hydrochar with recycled processing water, BioResources 8 (2013) 2981–2997.
[10] Z. Zhu, L. Rosendahl, S.S. Toor, D. Yu, G. Chen, Hydrothermal liquefaction of barley straw to bio-crude oil: effects of reaction temperature and aqueous phase recirculation, Appl. Energy 137 (2015) 183–192, https://doi.org/10.1016/j.apenergy.2014.10.005.
[11] D.C. Harris, Gas chromatography. Quantitative Chemical Analysis, 7th ed. ed., Freeman, New York, 2007, pp. 528–551.
[12] R.B. Madsen, M.M. Jensen, A.J. Mørup, K. Houlberg, P.S. Christensen, M. Klemmer, J. Becker, B.B. Iversen, M. Glasius, Using design of experiments to optimize derivatization with methyl chloroformate for quantitative analysis of the aqueous phase from hydrothermal liquefaction of biomass, Anal. Bioanal. Chem. 408 (2016) 2171–2183, https://doi.org/10.1007/s00216-016-9321-6.
[13] G.R. van der Hoff, P. van Zoonen, Trace analysis of pesticides by gas chromatography, J. Chromatogr. A 843 (1999) 301–322, https://doi.org/10.1016/S0021-9673(99)00511-7.
[14] R.B. Madsen, R.Z.K. Bernberg, P. Biller, J. Becker, B.B. Iversen, M. Glasius, Hydrothermal co-liquefaction of biomasses – quantitative analysis of bio-crude and aqueous phase composition, Sustain. Energy Fuels 1 (2017) 789–805, https://doi.org/10.1039/C7SE00104E.
[15] D.C. Harris, Hight-performance liquid chromatography. Quantitative Chemical Analysis, 7th ed. ed., Freeman, New York, 2007, pp. 556–584.
[16] R. Malviya, V. Bansal, O.P. Pal, P.K. Sharma, High performance liquid chromatography: a short review, J. Global Pharma Technol. 2 (2010) 22–26.
[17] W.J. Lough, I.W. Wainer, High Performance Liquid Chromatography: Fundamental Principles and Practice, Blackie Academic & Professional, London, 1995, p. 42.
[18] D.C. Harris, The analytical process. Quantitative Chemical Analysis, 7th ed. ed., Freeman, New York, 2007, pp. 1–7.
[19] G.D. Strahan, C.A. Mullen, A.A. Boateng, Characterizing biomass fast pyrolysis oils by 13C NMR and chemometric analysis, Energy Fuels 25 (2011) 5452–5461, https://doi.org/10.1021/ef2013166.
[20] N. Hao, H. Ben, C.G. Yoo, S. Adhikari, A.J. Ragauskas, Review of NMR characterization of pyrolysis oils, Energy Fuels 30 (2016) 6863–6880, https://doi.org/10.1021/acs.energyfuels.6b01002.
[21] N.S. Tessarolo, R.V.S. Silva, G. Vanini, A. Casilli, V.L. Ximenes, F.L. Mendes, A. de Rezende Pinho, W. Romão, E.V.R. de Castro, C.R. Kaiser, et al., Characterization of thermal and catalytic pyrolysis bio-oils by high-resolution techniques: 1H NMR, GC×GC-TOFMS and FT-ICR MS, J. Anal. Appl. Pyrolysis 117 (2016) 257–267, https://doi.org/10.1016/j.jaap.2015.11.007.
[22] A. Le Gresley, G. Broadberry, C. Robertson, J.-M.R. Peron, J. Robinson, S. O'Leary, Application of pure shift and diffusion NMR for the characterisation of crude and processed pyrolysis oil, J. Anal. App. Pyrolysis 140 (2019) 281–289, https://doi.org/10.1016/j.jaap.2019.04.005.
[23] M. Foroozandeh, G.A. Morris, M. Nilsson, PSYCHE pure shift NMR spectroscopy, Chem. Eur. J. 24 (2018) 13988–14000, https://doi.org/10.1002/chem.201800524.
[24] D.L. Pavia, Mass spectrometry - part one: basic theory, instrumentation and sampling techniques. Introduction to Spectroscopy, 5th ed., Cengage Learning, Stamford, Conn, 2015, pp. 107–138.
[25] U. Holzgrabe, Quantitative NMR spectroscopy in pharmaceutical applications, Prog. Nucl. Magn. Reson. Spectrosc. 57 (2010) 229–240, https://doi.org/10.1016/j.pnmrs.2010.05.001.
[26] U. Holzgrabe, R. Deubner, C. Schollmayer, B. Waibel, Quantitative NMR spectroscopy—applications in drug analysis, J. Pharm. Biomed. Anal. 38 (2005) 806–812, https://doi.org/10.1016/j.jpba.2005.01.050.
[27] T. Saito, T. Yamazaki, M. Numata, Development of nuclear magnetic resonance as a tool of quantitative analysis for organic materials, Metrologia 56 (2019), 054002.
[28] C. Løhre, J. Underhaug, R. Brusletto, T. Barth, Quantitative NMR-analysis of Aqueous Samples From Thermochemical Conversion of Biomass, 2020.
[29] S.K. Bharti, R. Roy, Quantitative 1H NMR spectroscopy, TrAC Trends Anal. Chem. 35 (2012) 5–26, https://doi.org/10.1016/j.trac.2012.02.007.
[30] F. Yue, C.M. Pedersen, X. Yan, Y. Liu, D. Xiang, C. Ning, Y. Wang, Y. Qiao, NMR studies of stock process water and reaction pathways in hydrothermal carbonization of furfural residue, Green Energy Environ. 3 (2018) 163–171, https://doi.org/10.1016/j.gee.2017.08.006.
[31] S. Ghoreishi, T. Barth, D.H.E. Hermundsgård, Ffect of reaction conditions on catalytic and noncatalytic lignin solvolysis in water media investigated for a 5 l reactor, ACS Omega 4 (2019) 19265–19278, https://doi.org/10.1021/acsomega.9b02629.
[32] H. Abdi, L.J.P. Williams, Rincipal component analysis, WIREs Computational Statistics 2 (2010) 433–459, https://doi.org/10.1002/wics.101.

[33] R. Carlson, J.E. Carlson, Chapter 2: experimental studies of reaction conditions. Initial remarks. Design and Optimization in Organic Synthesis, Elsevier, Amsterdam, 2005.
[34] S.G. Elliot, S. Tolborg, I. Sádaba, E. Taarning, S. Meier, Quantitative nmr approach to optimize the formation of chemical building blocks from abundant carbohydrates, ChemSusChem 10 (2017) 2990–2996.
[35] D.L. Pavia, Nuclear magnetic resonance spectroscopy - part one: basic concepts. Introduction to Spectroscopy, 5th ed., Cengage Learning, Stamford, Conn, 2015, pp. 215–289.
[36] Information, N.C.f.B. PubChem Database. Dimethyl ether (CID=8254), 2020. Availabe online: https://pubchem.ncbi.nlm.nih.gov/compound/Dimethyl-ether (accessed on accessed on Feb. 21,).
[37] M. Oregui-Bengoechea, I. Gandarias, P.L. Arias, T. Barth, Unraveling the role of formic acid and the type of solvent in the catalytic conversion of lignin: a holistic approach, ChemSusChem 10 (2017) 754–766, https://doi.org/10.1002/cssc.201601410.
[38] M. Oregui Bengoechea, N. Miletíc, M.H. Vogt, P.L. Arias, T. Barth, Analysis of the effect of temperature and reaction time on yields, compositions and oil quality in catalytic and non-catalytic lignin solvolysis in a formic acid/water media using experimental design, Bioresour. Technol. Rep. 234 (2017) 86–98, https://doi.org/10.1016/j.biortech.2017.02.129.
[39] ECN phyllis classification, Kraft Lignin From Eucalyptus, 2020. Availabe online: https://phyllis.nl/Biomass/View/944 (Accessed on 25. june).